

---

# 000 001 002 003 004 005 006 007 008 009 010 011 012 013 014 015 016 017 018 019 020 021 022 023 024 025 026 027 028 029 030 031 032 033 034 035 036 037 038 039 040 041 042 043 044 045 046 047 048 049 050 051 052 053 THE TAIL TELLS ALL: ESTIMATING MODEL-LEVEL MEMBERSHIP INFERENCE VULNERABILITY WITHOUT REFERENCE MODELS

Anonymous authors

Paper under double-blind review

## ABSTRACT

Membership inference attacks (MIAs) have emerged as the standard tool for evaluating the privacy risks of AI models. However, state-of-the-art attacks require training numerous, often computationally expensive, reference models, limiting their practicality. We present a novel approach for estimating model-level vulnerability, the TPR at low FPR, to membership inference attacks without requiring reference models. Empirical analysis shows loss distributions to be asymmetric and heavy-tailed and suggests that most points at risk from MIAs have moved from the tail (high-loss region) to the head (low-loss region) of the distribution after training. We leverage this insight to propose a method to estimate model-level vulnerability from the training and testing distribution alone: using the absence of outliers from the high-loss region as a predictor of the risk. We evaluate our method, the TNR of a simple loss attack, across a wide range of architectures and datasets and show it to accurately estimate model-level vulnerability to the SOTA MIA attack (LiRA). We also show our method to outperform both low-cost (few reference models) attacks such as RMIA and other measures of distribution difference. We finally evaluate the use of non-linear functions to evaluate risk and show the approach to be promising to evaluate the risk in large-language models.

## 1 INTRODUCTION

Large-scale machine learning systems have seen rapid adoption across healthcare, finance, legal, and other domains in recent years, with many models now being fine-tuned on sensitive and confidential data. A large body of research has however shown that these models may inadvertently memorize certain samples within their training data (often outliers) (Carlini et al., 2019; 2022b), raising strong privacy concerns.

Membership inference attacks (MIAs) have become the primary tool to measure the empirical privacy leakage of a model, evaluating the practical risk and providing a bound on the success of other types of attacks (Ponomareva et al., 2023). The privacy risk of a model is quantified by the attack’s True Positive Rate (TPR) at a low False Positive Rate (FPR) (Carlini et al., 2022a; Watson et al., 2021; Ye et al., 2022; Zarifzadeh et al., 2023), focusing on the members an attack can confidently infer. This is also aligned with legal requirements, such as EU GDPR “reasonably likely” standard for singling out and the UK Information Commissioner’s Office’s recent guidance (European Data Protection Board, 2024; , ICO).

### 1.1 PROBLEM STATEMENT

The most effective MIAs, such as the Likelihood Ratio Attack (LiRA), however require training tens to hundreds of reference models, each requiring computational resources equivalent to the original model. The low loss of a sample on its own can be caused by both generalization and memorization. State-of-the-art MIAs are believed to mainly use reference models to distinguish between the two. It has also been shown that the success of an attack increases with the number of reference models, with recent work showing continuous improvement with 256 reference GPT-2 models (Hayes et al., 2025), and that reference models need to be trained with the same architecture and setup as the model under attack to be optimal (Carlini et al., 2022a; Zarifzadeh et al., 2023). The high computational

054 cost of SOTA attacks limits their practicality as privacy risk evaluation tools, especially for complex models and LLMs. Importantly, this cost becomes even more prohibitive in realistic workflows 055 such as hyperparameter and architecture selection, where practitioners must compare privacy-utility 056 tradeoffs across many training configurations Ponomareva et al. (2023), as well as continuous monitoring 057 of routinely retrained production models and rapid pre-deployment risk assessments. All of 058 these settings require evaluating numerous candidate models without incurring the computational 059 overhead of training new reference models for every iteration.

060 A recent line of research has aimed to decrease the number of reference models needed to perform 061 attacks. The state-of-the-art for this, RMIA, however still requires the training of at least one reference 062 model (Zarifzadeh et al., 2023). Another line of research focused instead on methods to score 063 the vulnerability of individual training samples to MIAs. These however do not provide an overall 064 model-level risk metric (Leemann et al., 2024; Pollock et al., 2025).

065 **We here propose a new approach and method to estimate the vulnerability of a model to state- 066 of-the-art membership inference attacks, leveraging new insights and using metrics available 067 with no additional training.**

## 070 1.2 OUR APPROACH: MEASURING WHAT'S MISSING

071 Membership inference attacks take advantage of the fact that models tend to be more confident 072 and exhibit lower loss in their predictions for data samples they have seen during training. This 073 differential behavior is a direct consequence of the optimization process that aims to minimize the 074 loss with some samples being more difficult to learn than others due to their difficulty, rarity or 075 position as outliers in the dataset distribution and being memorized.

076 We study train and test loss distributions across a wide range of setups and observe empirically that 077 loss distributions tend to be asymmetric and heavy-tailed, with most samples having a near zero loss 078 whilst a few have a much higher loss than average. We posit that the heavy tail of the test set's 079 distribution, compared to that of the train set, is due to samples from the training set's distribution 080 that should have a high loss (hard example) but have shifted to the low-loss region during training, 081 having been effectively memorized.

082 These observations are in line with the literature and explain a well-known fact: the LOSS attack 083 (Yeom et al., 2018) often achieves poor TPR@low FPR values despite a relatively high AUC.

084 We also posit and empirically confirm across a wide variety of setups that samples missing from 085 the tail of the training set distribution (high loss) constitute a significant fraction of the samples 086 ultimately deemed to be most vulnerable to SOTA reference model-based MIAs.

087 Leveraging these insights, we propose a class of methods to estimate the model-level risk to SOTA 088 MIAs from readily available train and test set loss distributions, measuring the absence of samples 089 from the train distribution to estimate risks. In particular we show the TNR of the loss attack, its 090 known ability to confidently identify non-members, to provide an accurate estimate of model-level 091 risk.

## 095 2 PRELIMINARIES

### 098 2.1 NOTATION

100 We denote with  $f_\theta : \mathcal{X} \rightarrow \mathcal{Y}$  a machine learning classification model parameterized by  $\theta$ , with input 101 space  $\mathcal{X}$  and output space  $\mathcal{Y} = [0, 1]^n$ . Model  $f_\theta \leftarrow \mathcal{T}(D_{\text{train}})$  is trained on dataset  $D_{\text{train}} \sim \mathcal{X} \times \mathcal{Y}$  102 using algorithm  $\mathcal{T}$  and loss function  $\ell$ . A separate test dataset  $D_{\text{test}} \sim \mathcal{X} \times \mathcal{Y}$  is reserved for 103 evaluation and is never used during training. For sample  $(x, y)$ , we write  $f_\theta(x)_y$  for the predicted 104 probability for class  $y$  and  $\ell(x, y) = \ell(f_\theta(x)_y, y)$  for the corresponding loss.

105 Membership inference attacks (MIAs) aim to determine whether a given record  $(x, y)$  was used to 106 train target model  $f_\theta$ . Specifically, given target model  $f_\theta$  and target record  $(x, y) \in \mathcal{X} \times \mathcal{Y}$ , an MIA 107  $A(x, y, f_\theta)$  aims to infer whether  $(x, y) \in D_{\text{train}}$  ( $(x, y)$  is a member) or not ( $(x, y)$  is a non-member). 108 We denote the target model's loss on  $(x, y)$  with  $\ell_{\text{target}}(x, y)$ . The attack outputs a membership score

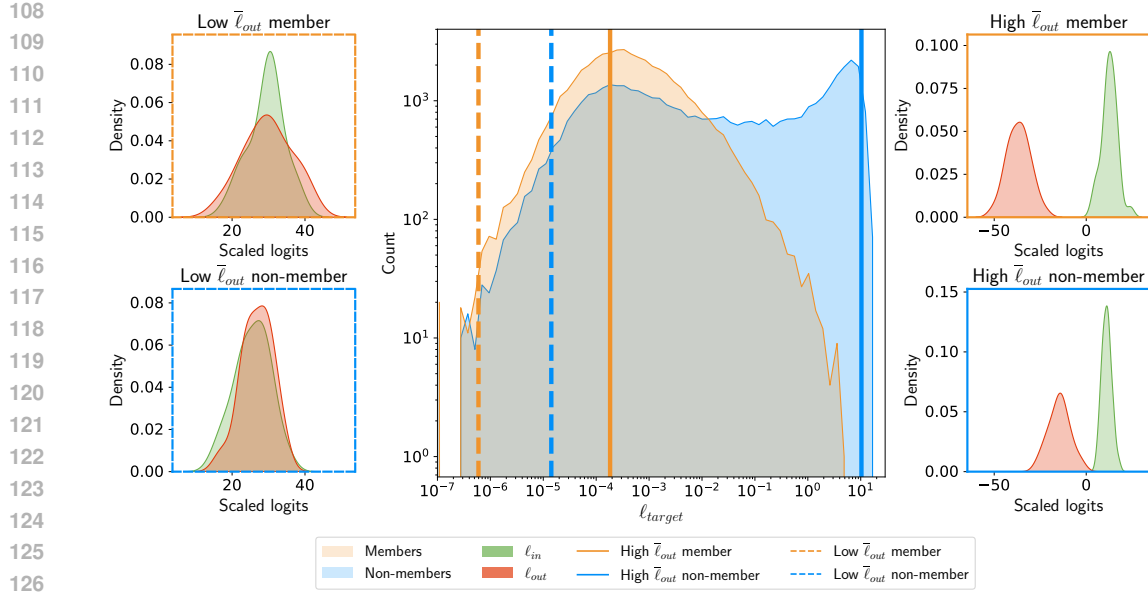


Figure 1: **Vulnerable members are mostly those that moved from tail to head.** The central panel shows member (orange) and non-member (blue) loss distributions on the target model. **Non-members dominate the high-loss tail** (right side), while members concentrate at low loss. Vertical lines mark  $\ell_{target}$  values for representative sample groups. Side panels display the IN and OUT scaled logit distributions that LiRA uses to compute membership scores for these samples: left panels show samples with low  $\ell_{out}$ , right panels show samples with high  $\ell_{out}$ . In particular, note how the **LiRA-vulnerable members** (orange solid line, top-left panel) have low  $\ell_{target}$  but high  $\ell_{out}$  indicating these samples would naturally fall in the high-loss tail but moved to the low-loss  $\ell_{target}$  head through training. Results shown are for ResNet-18 trained on CINIC-10.

that quantifies the likelihood of the target sample  $(x, y)$  being part of the training data of the target model. The attacker then makes a binary membership prediction according to threshold  $\tau$ :

$$A_\tau(x, y, f_\theta) = \begin{cases} 1 & \text{if } A(x, y, f_\theta) \geq \tau \\ 0 & \text{otherwise} \end{cases} \quad (1)$$

A simple and widely used example is the LOSS attack  $A_{\text{LOSS}}$  (Yeom et al., 2018), where a sample's membership score is the loss of the target model on it and  $\mathbb{1}$  is the indicator function:

$$A_{\text{LOSS}}(x, y) = \mathbb{1}[-\ell_{\text{target}}(x, y) > \tau] \quad (2)$$

We report the model-level risk as the True Positive Rate (TPR) at a fixed False Positive Rate (FPR)= $\alpha$  (Carlini et al., 2022a; Ye et al., 2022; Zarifzadeh et al., 2023) of an attack.

SOTA attacks rely on *reference models*, models trained on auxiliary datasets  $D_{\text{reference}} \sim \mathcal{X} \times \mathcal{Y}$  using the same architecture and training process as the target model. For a sample  $(x, y)$ , an “OUT” reference model  $f_{\theta_{\text{OUT}}}$  is trained on data excluding  $(x, y)$ , while an “IN” reference model  $f_{\theta_{\text{IN}}}$  is trained with it. This distinction enables the attacker to compare model behavior in the presence and absence of the target sample, improving its power. For a sample  $(x, y)$ , we denote with  $\ell_{\text{OUT}}(x, y)$  the loss of an OUT model on  $(x, y)$ , and analogously for an IN model. For  $K$  IN reference models, we define the mean loss:

$$\bar{\ell}_{\text{in}}(x, y) = \frac{1}{K} \sum_{k=1}^K \ell(f_{\text{IN}}^k(x, y)) \quad (3)$$

---

162 and analogously for  $\bar{\ell}_{out}(x, y)$ .  
163

164 **2.2 SOTA REFERENCE MODEL-BASED MEMBERSHIP INFERENCE ATTACKS**  
165

166 The current state-of-the-art reference-model based attack is the Likelihood Ratio Attack  
167 (LiRA) (Carlini et al., 2022a). It estimates the loss distributions of models trained with and without  
168 a target sample  $(x, y)$ , and computes their likelihood ratio as a membership score. In the *online*  
169 attack, the attacker trains both “IN” and “OUT” reference models, and in the more efficient *offline*  
170 version, only trains “OUT” models. We adopt the strongest online attack in our experiments.

171 Recent work has explored methods to reduce the number of reference models needed for an effective  
172 attack. The state-of-the-art approach in this setting is RMIA (Zarifzadeh et al., 2023). It computes  
173 membership scores by comparing the target sample to samples sampled from the population using  
174 simple pairwise tests, and has been shown to outperform LiRA when few reference models are  
175 available. We compare our method to it.

177 **3 EXPERIMENTAL SETUP**  
178

179 **Datasets.** We select 4 image classification datasets widely used in the literature: MNIST, CIFAR-  
180 10, CINIC-10 and CIFAR-100. MNIST contains 70,000 grayscale 28×28 images of handwritten  
181 digits (0-9). CIFAR-10 has 60,000 32×32 color images across 10 natural object classes, and CINIC-  
182 10 combines CIFAR-10 with downsampled ImageNet data, creating 270,000 32×32 images across  
183 the same 10 classes as CIFAR-10 but with greater data volume and diversity. Finally, CIFAR-100  
184 contains the same images as CIFAR-10, but is divided into 100 fine-grained classes.

185 **Models.** We train 9 neural network architectures commonly used for image classification, ranging  
186 between 60K and 172M parameters on all 4 datasets: ResNet-20 (He et al., 2016), WRN28-  
187 2 (Zagoruyko & Komodakis, 2016), MobileNetV2 (Sandler et al., 2018), DenseNet121 (Huang  
188 et al., 2017), WRN40-4, ResNet-18, WRN28-10, VGG11 and VGG16 (Simonyan & Zisserman,  
189 2015). [Additionally, we finetune ViT-B-16 pretrained on ImageNet on CIFAR-10](#). We follow the  
190 setup from Carlini et al. (2022a) where each model is trained on a randomly selected subset  
191 consisting of 50% of the samples from the training split as “members,” with the other 50% reserved  
192 as non-members using regularization methods including weight decay and data augmentation to  
193 achieve a high training accuracy of over 90%. We use stochastic gradient descent as the optimizer  
194 with a cosine annealing learning rate schedule and a batch size of 256. Models are trained for 50 to  
195 200 epochs depending on the complexity of the dataset and the size of the model.

196 **Attacks.** We instantiate LiRA and RMIA in the “online” setting with 64 reference models, comprising  
197 32 IN and 32 OUT models. We follow the “mirror” setup from Carlini et al. (2022a) using 2  
198 augmentations.

200 For the LOSS attack, we collect per-sample loss values at the final epoch of training for the target  
201 model.

203 **4 INTUITION**  
204

205 **Loss distributions are heavy-tailed.** Figure 1 shows the member and non-member target model  
206 loss distributions on a semilog scale for ResNet-18 on CINIC-10; complete results are shown in  
207 Appendix A. In both cases, most probability mass lies at low loss (the “head”), with a smaller  
208 fraction at high loss (the “tail”). For members, the head corresponds to learned or memorized  
209 examples, while the tail comprises harder-to-learn samples (Pollock et al., 2025). For non-members,  
210 the head reflects samples the model generalizes to, whereas the tail contains difficult or outlier cases  
211 that the model fails to fit.

212 **The difference between member and non-member loss distributions is driven by the tail.** The  
213 member and non-member distributions differ in mean but overlap substantially in the low-loss re-  
214 gion. The meaningful separation arises in the high-loss tail, where the non-member distribution  
215 places much more mass than the member distribution.

216 During the optimization process, gradient updates are likely larger for high-loss training examples;  
 217 training pushes these extreme member losses into the low-loss region, shrinking the member tail  
 218 rather than uniformly lowering all losses.

219 Because this tail is composed almost entirely of  
 220 high-loss non-members, the LOSS attack can  
 221 identify these samples with high confidence.

223 **Vulnerable members are those that are miss-  
 224 ing from the tail.** The non-member distri-  
 225 bution reflects the model’s behavior on un-  
 226 seen data. Assuming that members and non-  
 227 members are drawn i.i.d. from the same under-  
 228 lying distribution, the absence of a heavy tail  
 229 for members then suggests that samples which  
 230 would be in the high-loss region, had they not  
 231 been seen by the model during training, have  
 232 shifted into the low-loss region. These mem-  
 233 bers now fall into the head of the distribution,  
 234 where they are difficult to distinguish from easy  
 235 non-members.

236 State-of-the-art membership inference attacks  
 237 such as LiRA target exactly these members. We  
 238 therefore hypothesize that the members most  
 239 vulnerable to LiRA are mainly these tail-to-  
 240 head samples. Figure 1 supports this hypoth-  
 241 esis: samples with the highest LiRA scores ex-  
 242 hibit low target-model losses, yet the  $\bar{\ell}_{out}$  is  
 243 high and aligns with the heavy tail of the non-  
 244 member distribution (see Appendix A for re-  
 245 sults for all setups). This pattern indicates that  
 246 training shifted these examples from the tail to the head. [We provide a formal explanation of this intuition in Appendix B.](#)

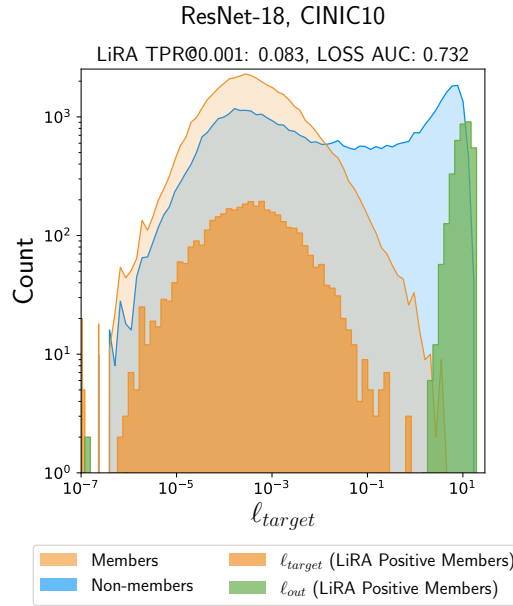
## 248 5 ESTIMATING VULNERABILITY TO SOTA MIAs

250 Leveraging these insights, we propose a new approach and method to evaluate model-level risk to  
 251 SOTA MIAs that does not require expensive reference model training: measuring the “missing”  
 252 member records. In particular, we propose to estimate model-level risk using the True Negative  
 253 Rate (TNR) at a fixed FPR of the LOSS attack. The TNR measures how good the LOSS attack is at  
 254 confidently identifying non-members, providing a measure of how “separable” the tail is from the  
 255 member distribution. For a set of non-members  $D_{test}$ , model  $f_\theta$  and threshold  $\tau$ , we compute the  
 256 LOSS TNR as the fraction of correctly identified non-members:

$$258 \text{TNR}_{\text{LOSS}}(D_{\text{test}}, f_\theta, \tau) = \frac{|\{A_{\text{LOSS}}(f_\theta, x, y) > \tau | (x, y) \in D_{\text{test}}\}|}{|D_{\text{test}}|} \quad (4)$$

261 We select  $\tau$  to achieve a False Negative Rate equal to the FPR of the LiRA attack for which we  
 262 are estimating the TPR. In line with the literature, we focus on FPR=0.001, but present results for  
 263 different FPR values (see Appendix B). [We select FNR=FPR as the most natural choice, but show our method is robust to the choice of FNR threshold: as shown in Appendix B, LOSS TNR maintains strong predictive performance across a wide range of FNR values, with RMSE remaining relatively stable.](#)

267 Figure 3 shows the LOSS TNR to be a very good predictor of LiRA’s TPR@FPR=10<sup>-3</sup> across  
 268 models and datasets, obtaining a low RMSE of 0.03 with a simple linear predictor with one param-  
 269 eter (we fix the y-intercept to be 0 as we expect a LOSS TNR of 0 to result in a LiRA TPR of 0).  
 Bootstrapping with 1000 iterations provides narrow confidence intervals, confirming that the linear



257 Figure 2: Loss distributions for members and  
 258 non-members for ResNet-18 (CINIC10). Or-  
 259 ange histogram shows member losses, blue shows  
 260 non-member losses, with density curves overlaid.  
 261 Green bars indicate the OUT model mean ( $\mu_{out}$ )  
 262 for points identified by LiRA at FPR=0.001.  
 263 [We provide a formal explanation of this intuition in Appendix B.](#)

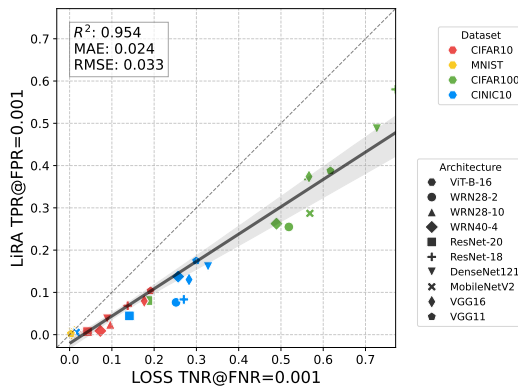


Figure 3: LOSS TNR reliably predicts LiRA TPR@FPR=0.001 across varied model architectures and datasets. The linear relationship (solid black line) exhibits strong performance with RMSE=0.033. The 97.5% confidence interval is shown as the shaded region.

Table 1: Performance metrics for LOSS TNR@0.001 as a predictor of LiRA TPR@0.001. Results are averaged across datasets and architectures reported in Section 3.

Metric	R <sup>2</sup>	RMSE	MAE
LOSS TNR (Ours)	<b>0.954</b>	<b>0.032</b>	<b>0.024</b>
Train-Test Gap	0.717	0.081	0.060
LT-IQR AUC	0.806	0.067	0.046
Loss AUC	0.844	0.051	0.052
RMIA (2 reference models)	0.910	0.046	0.036

model maintains a high degree of certainty over the full range of values. This allows practitioners to accurately estimate the LiRA TPR@FPR without reference models. [This is particularly useful for many scenarios that require evaluating many candidate models such as hyperparameter tuning, neural architecture search, or comparing training strategies.](#)

We then compare our approach against an alternate metric, (i) LOSS attack AUC, and baselines: (ii) train-test accuracy gap of the target model; and (iii) LT-IQR AUC (Pollock et al., 2025). LT-IQR is the SOTA for identifying the samples most at risk to LiRA, but is not a measure of overall model vulnerability.

Table 1 reports goodness-of-fit metrics for linear functions fit on our approach and baselines and show it to outperform the baselines and to be a good estimator of vulnerability to LiRA.

Aware of the prohibitive cost of SOTA MIA methods, a recent line of research aims to develop low-costs attacks which can be used by model developers to estimate the model-level risk. We also instantiate the SOTA low-cost attack, online RMIA, with two reference models and compare its predictive power to our method.

As shown in Table 1, our method outperforms RMIA at estimating LiRA TPR, despite RMIA requiring at least 2 reference models.

LOSS AUC, which measures distributional separability across all loss values, would be more effective if memorization were evenly distributed. The train-test gap, a metric studied in the literature, captures only mean differences between loss distributions. While it performs moderately well, we observe that it cannot detect tail differences caused by the asymmetric non-member distribution.

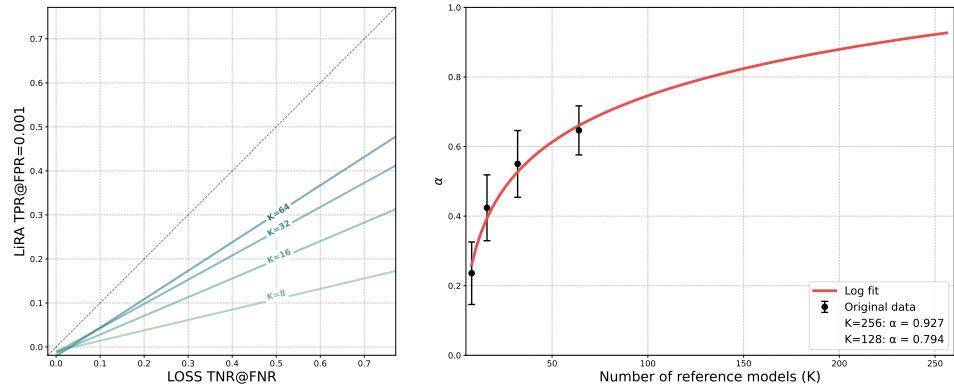


Figure 4: Performance of linear models for predicting LiRA with varying numbers of reference models (K). Left panel shows the correlation between LOSS TNR (x-axis) and LiRA TPR@0.001 (y-axis) across different K values, with linear regression fits shown for each condition. Right panel shows slope parameter ( $\alpha$ ) for different K. The error bars show the 97.5% confidence intervals obtained with bootstrapping.

### 5.1 VARYING THE NUMBER OF REFERENCE MODELS

We study the effectiveness of LOSS TNR at estimating the TPR@FPR of attacks of varying strength. We instantiate LiRA with 4, 8, 16, 32 and 64 reference models and report the resulting linear model for each value of K, along with the slopes  $\alpha$ .

Figure 4 shows the risk to steadily increase with K as the attack becomes more confident at identifying members. As noticed in previous work though, TPR@low FPR experiences decreasing returns as the number of reference models increase which we can now model to estimate the risk against stronger attackers.

### 5.2 FITTING DIFFERENT FUNCTIONS

We have so far estimated LiRA TPR with a simple linear model. We now study whether non-linear models lead to better risk estimates. Identifying non-members is indeed a matter of finding a good threshold to separate the tail of the loss distribution from the rest, while identifying members is dependent on reference models and is likely to be a more difficult task. We indeed find empirically that the LOSS TNR is typically higher than LiRA TPR at the same FPR.

We thus compute goodness-of-fit metrics for convex functions such as a two-parameter polynomial, power-law, and exponential functions.

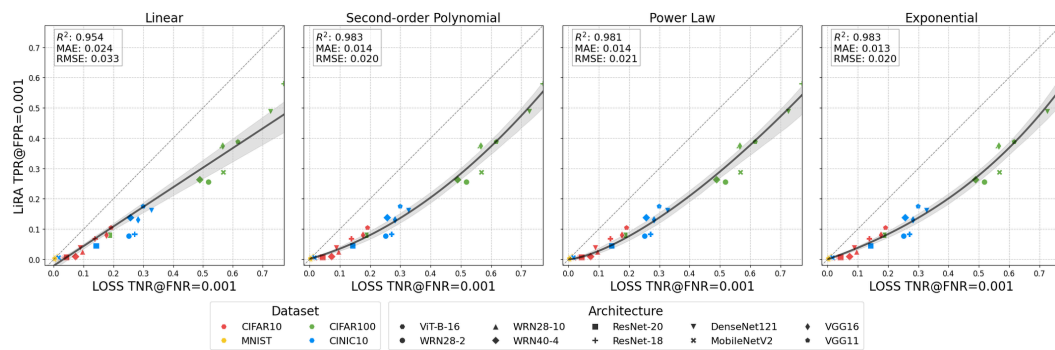


Figure 5: Comparison of regression models for predicting TPR@0.001 with LOSS TNR@0.001 evaluated on image recognition setups. The exponential function achieves the lowest RMSE of 0.02, compared to 0.033 achieved by the linear fit.

378 Figure 5 shows that the exponential function  $a(e^{bx} - 1)$  achieves the best fit, outperforming the  
 379 linear model. An exponential fit would imply that as LOSS TNR increases, member identification  
 380 becomes easier as the model memorizes more difficult samples. Initial gains in LOSS TNR produce  
 381 modest improvements in LiRA TPR, but these improvements accelerate as memorization increases.  
 382  
 383  
 384

### 385 5.3 ROBUSTNESS ACROSS LEVELS OF GENERALIZATION GAPS

386 Prior work has identified overfitting, typically  
 387 measured by the train-test accuracy gap, as a  
 388 key factor influencing membership inference  
 389 vulnerability (Carlini et al., 2022a; Yeom et al.,  
 390 2018).

391 We now study the effectiveness of our method  
 392 for predicting the vulnerability of models with  
 393 widely varying train-test gaps, ranging from  
 394 near-zero (minimal overfitting) to over 50 per-  
 395 centage points (severe overfitting). Specifically,  
 396 we treat intermediate training checkpoints from  
 397 each setup in our main experiment as additional  
 398 target models, instantiate LiRA against each  
 399 target, and assess how well our method predicts  
 400 its vulnerability. Figure 6 shows that LOSS  
 401 TNR remains a reliable predictor of model vul-  
 402 nerability across this full range of generaliza-  
 403 tion gaps.

404 This consistency demonstrates that LOSS TNR  
 405 captures memorization patterns much richer than that of the overall generalization performance.  
 406 While models with larger train-test gaps tend to have higher vulnerability (evidenced by the color  
 407 gradient), TNR provides accurate risk estimates across a wide spectrum.

### 408 5.4 LLMs

410 Recent evidence suggests that LLMs exhibit fundamentally different memorization patterns than  
 411 traditional models. The size of LLMs, for instance, allows them to achieve excellent generalization  
 412 while simultaneously memorizing training data (Tirumala et al., 2022). The nature of their training  
 413 data also makes them subject to what Shilov et al. (2024) describe as “mosaic memory”, the ability  
 414 of LLMs to memorize fuzzy duplicates in their training data, rather than exact samples.

415 Given the importance of the task, however, we test our approach on LLMs. Following the setup  
 416 proposed in recent work Hayes et al. (2025), we evaluate our method on 5 GPT-2 models with 10M,  
 417 104M, 302M, 604M, and 1018M parameters. We train each model on a  $2^{19}$ -sample subset of the C4  
 418 dataset and instantiate online LiRA with 256 reference models (128 IN, 128 OUT).

419 While more traditional image and other models show discrete, example-specific memorization that  
 420 creates clear distributional differences and asymmetric, heavy-tailed distributions, LLMs show loss  
 421 distributions that are much more symmetrical, with little difference between the train and test distri-  
 422 butions even when models can be shown to have memorized training data. TNR is therefore not an  
 423 appropriate risk estimator in this setting.

424 However, we posit that LOSS AUC, as a more general estimate of “missing records”, may provide  
 425 an accurate estimation of model-level risk. Fig.7 shows it to indeed be a good estimator of the risk,  
 426 obtaining an RMSE of 0.01.

## 428 6 RELATED WORK

431 **Membership inference attacks.** MIAs aim to infer whether a data sample was used to train a  
 given target model. Homer et al. (2008) originally introduced membership inference attacks (MIA)

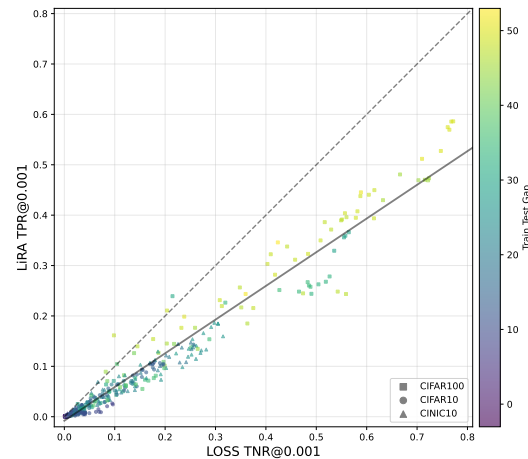


Figure 6: LOSS TNR reliably predicts LiRA TPR across varying overfitting levels.

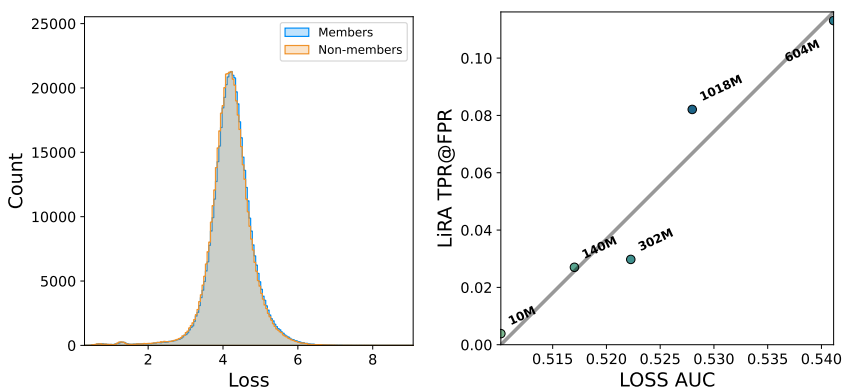


Figure 7:  $\ell_{target}$  distributions and predictive relationship for large language models. Left:  $\ell_{target}$  distributions for members (blue) and non-members (orange) show high overlap and symmetry, unlike the asymmetric, heavy-tailed distributions observed in image classification models (Figure 1). Right: Despite symmetric distributions, LOSS AUC reliably predicts LiRA TPR@FPR=0.001 across five GPT-2 models (10M to 1018M parameters), achieving RMSE=0.01. Points are labeled by model size.

to identify the presence of an individual’s genome data among aggregate summary statistics. (Shokri et al., 2017) proposed the first MIA on machine learning models and demonstrated their efficacy in the black-box setting. MIAs have since become the de-facto standard to empirically measure the privacy risk posed by a model and providing an upper bound on the risk of more severe empirical attacks such as attribute inference or model inversion (Fredrikson et al., 2015).

Simple MIAs compare metrics like loss Yeom et al. (2018) or confidence Song et al. (2019) against thresholds, while others Mattern et al. (2023) compare samples against neighboring samples. While these attacks can obtain high AUC values, they have been shown to be unable to confidently identify members as they struggle to distinguish between low-loss samples that have been memorized and those that are easy to predict. Difficulty-calibrated attacks (He et al., 2024; Song & Mittal, 2020; Watson et al., 2021) aim to address this but still lack high confidence.

State-of-the-art attacks rely on reference models Shokri et al. (2017) to calibrate the attack with respect to sample difficulty. The Likelihood Ratio Attack (LiRA)(Carlini et al., 2022a) estimates loss distributions for IN and OUT models and performs a likelihood ratio test to determine membership of a given sample. Other methods such as Attack R use only OUT reference models (Ye et al., 2022), while others employ knowledge distillation to train reference models (Li et al., 2024; Liu et al., 2022).

**Low-cost attacks and free identification of vulnerable samples.** Reference model-based attacks depend heavily on the number and quality of reference models. On CIFAR-10, LiRA TPR@0.01% drops from 2.83% with 254 reference models to 0.76% with 4 (Zarifzadeh et al., 2023). Performance declines further with fewer models or smaller or mismatched architectures. In practice, dozens to hundreds of identical reference models are often needed for high accuracy, making these attacks difficult to scale to iterative workflows and large-scale models such as LLMs (Carlini et al., 2022a).

Recent work has explored ways to estimate model vulnerability to LiRA at lower computational cost or even for free. The state-of-the-art low-cost attack, RMIA (Zarifzadeh et al., 2023), combines reference models with population samples to construct an attack they show to match LiRA performance with as few as 2 reference models. Quantile regression-based attacks (Bertran et al., 2023) use a single regression model to match LiRA’s TPR, but their effectiveness is limited to scenarios with only one reference model.

Another direction of research focuses on free identification of the samples that are most vulnerable to SOTA reference model-based MIAs. Predictors such as sample loss, confidence, and training loss dynamics have been shown to successfully identify highly vulnerable samples (Leemann et al., 2024; Pollock et al., 2025) for free. In particular, LT-IQR has been shown to achieve high precision

486 at identifying samples vulnerable to LiRA (Pollock et al., 2025). These methods, however, do not  
487 readily provide model-level risk scores as their outputs are inherently relative.  
488

489 **Factors influencing membership inference vulnerability.** Previous work has explored the  
490 connection between a model’s training and its vulnerability to MIAs. Yeom et al. (2018) proposed  
491 overfitting as a sufficient but not necessary condition for MIA success, whilst other works demon-  
492 strate a correlation between the train-test gap (a measure of overfitting) and MIA success (Carlini  
493 et al., 2022a; Yeom et al., 2018). Other work has studied the impact of dataset properties on model  
494 vulnerability: models trained on smaller datasets are more vulnerable (Chen et al., 2020; Németh  
495 et al., 2025; Tobaben et al., 2025), and, within a dataset, classes with fewer samples contain more  
496 vulnerable examples (Chang & Shokri, 2021; Kulynych et al., 2022).

## 497 7 CONCLUSION

498

500 We present a novel method to estimate model-level vulnerability to SOTA membership inference  
501 attacks without reference models. We show a significant fraction of highly vulnerable samples  
502 being samples that are “missing” from the tail of the training distribution and instead moved to the  
503 low loss head of the distribution. We propose to use the LOSS attack, and in particular its TNR, to  
504 quantify the missing samples and estimates the model’s vulnerability to LiRA.

505 Across 9 architectures and 4 datasets, we show our method to achieves an RMSE of 0.032 in predict-  
506 ing the LiRA TPR@FPR=0.001 with similar results for other FPR values. Our method outperforms  
507 other measures including train-test accuracy gap and LT-IQR, as well as recent low-cost attacks at  
508 estimating model-level risk. We also test non-linear risk estimation models and show the method to  
509 enable model developer to estimate the risk posed by strong attackers willing to train a large number  
510 of reference models. **Our method is robust to the generalization gap of the target model, and also to**  
511 **the choice of FNR threshold.**

512 Finally, given the importance of the task, we apply our approach to LLMs. While they are know  
513 to exhibit different memorization pattern, we show LOSS AUC might still serve as an effective  
514 estimation of model-level vulnerability to SOTA reference model-based MIAs.

515 Taken together, our work provides a novel practical approach to estimating model-level vuln-  
516 erability to SOTA attacks with no additional computational cost. Where SOTA attacks often require  
517 training hundreds of reference models, our method uses only the target model’s loss values. We be-  
518 lieve this will greatly help enable privacy risk assessments in practice, in particular during iterative  
519 development workflows and **scenarios where multiple candidate models require assessment.**

520 **Limitations and future work.** We evaluate in the work the use of LOSS TNR (and AUC) to  
521 estimate model vulnerability to LiRA. While LiRA is the state-of-the-art and has been shown to  
522 outperform other approaches, we have not assessed the transferability of our method to other MIAs  
523 or to broader privacy threats (e.g., reconstruction or inversion). While we test it on a range of  
524 setups (datasets and architectures) covering a range of risk level, TNR is an estimator of the risk  
525 and there might be cases where our results do not generalize. Due to computational constraints, our  
526 LLM study spans five mid-sized architectures. Evaluating scaling to larger models and datasets and  
527 sensitivity to training regimes are natural next steps.

## 528 REFERENCES

529

531 Martin Bertran, Shuai Tang, Aaron Roth, Michael Kearns, Jamie H Morgenstern, and Steven Z Wu.  
532 Scalable membership inference attacks via quantile regression. *Advances in Neural Information  
533 Processing Systems*, 36:314–330, 2023.

534 Nicholas Carlini, Chang Liu, Úlfar Erlingsson, Jernej Kos, and Dawn Song. The secret sharer:  
535 Evaluating and testing unintended memorization in neural networks. In *28th USENIX security  
536 symposium (USENIX security 19)*, pp. 267–284, 2019.

538 Nicholas Carlini, Steve Chien, Milad Nasr, Shuang Song, Andreas Terzis, and Florian Tramer. Mem-  
539 bership inference attacks from first principles. In *2022 IEEE symposium on security and privacy  
(SP)*, pp. 1897–1914. IEEE, 2022a.

540 Nicholas Carlini, Andreas Terzis, Matthew Jagielski, Florian Tramer, Nicolas Papernot, and Chiyuan  
541 Zhang. The privacy onion effect: memorization is relative. In *Proceedings of the 36th Interna-*  
542 *tional Conference on Neural Information Processing Systems*, NIPS '22, Red Hook, NY, USA,  
543 2022b. Curran Associates Inc. ISBN 9781713871088.

544 Hongyan Chang and Reza Shokri. On the privacy risks of algorithmic fairness. In *2021 IEEE*  
545 *European Symposium on Security and Privacy (EuroS&P)*, pp. 292–303. IEEE, 2021.

546 Dingfan Chen, Ning Yu, Yang Zhang, and Mario Fritz. Gan-leaks: A taxonomy of membership  
547 inference attacks against generative models. In *Proceedings of the 2020 ACM SIGSAC Conference*  
548 *on Computer and Communications Security*, CCS '20, pp. 343–362, New York, NY, USA, 2020.  
549 Association for Computing Machinery. ISBN 9781450370899. doi: 10.1145/3372297.3417238.  
550 URL <https://doi.org/10.1145/3372297.3417238>.

551 European Data Protection Board. Opinion 28/2024 on certain data protection aspects related to  
552 the processing of personal data in the context of ai models. Adopted on 17 December 2024,  
553 December 2024. URL [https://www.edpb.europa.eu/system/files/2024-12/edpb\\_opinion\\_202428\\_ai-models\\_en.pdf](https://www.edpb.europa.eu/system/files/2024-12/edpb_opinion_202428_ai-models_en.pdf). Version 1.0.

554 Matt Fredrikson, Somesh Jha, and Thomas Ristenpart. Model inversion attacks that exploit confi-  
555 dence information and basic countermeasures. In *Proceedings of the 22nd ACM SIGSAC Conference*  
556 *on Computer and Communications Security*, CCS '15, pp. 1322–1333, New York, NY, USA,  
557 2015. Association for Computing Machinery. ISBN 9781450338325. doi: 10.1145/2810103.  
558 2813677. URL <https://doi.org/10.1145/2810103.2813677>.

559 Jamie Hayes, Ilia Shumailov, Christopher A. Choquette-Choo, Matthew Jagielski, George Kaassis,  
560 Katherine Lee, Milad Nasr, Sahra Ghalebikesabi, Niloofar Mireshghallah, Meenatchi Sundaram  
561 Mutu Selva Annamalai, Igor Shilov, Matthieu Meeus, Yves-Alexandre de Montjoye, Franziska  
562 Boenisch, Adam Dziedzic, and A. Feder Cooper. Strong membership inference attacks on massive  
563 datasets and (moderately) large language models, 2025. URL <https://arxiv.org/abs/2505.18773>.

564 Kaiming He, Xiangyu Zhang, Shaoqing Ren, and Jian Sun. Deep residual learning for image recog-  
565 nition. In *Proceedings of the IEEE conference on computer vision and pattern recognition*, pp.  
566 770–778, 2016.

567 Yu He, Boheng Li, Yao Wang, Mengda Yang, Juan Wang, Hongxin Hu, and Xingyu Zhao. Is  
568 difficulty calibration all we need? towards more practical membership inference attacks, 2024.  
569 URL <https://arxiv.org/abs/2409.00426>.

570 Nils Homer, Szabolcs Szelinger, Margot Redman, David Duggan, Waibhav Tembe, Jill Muehling,  
571 John V Pearson, Dietrich A Stephan, Stanley F Nelson, and David W Craig. Resolving individuals  
572 contributing trace amounts of dna to highly complex mixtures using high-density snp genotyping  
573 microarrays. *PLoS genetics*, 4(8):e1000167, 2008.

574 Gao Huang, Zhuang Liu, Laurens Van Der Maaten, and Kilian Q Weinberger. Densely connected  
575 convolutional networks. In *Proceedings of the IEEE conference on computer vision and pattern*  
576 *recognition*, pp. 4700–4708, 2017.

577 Information Commissioner's Office (ICO). How should we assess secu-  
578 rity and data minimisation in ai?, 2025. URL <https://ico.org.uk/for-organisations/uk-gdpr-guidance-and-resources/artificial-intelligence/guidance-on-ai-and-data-protection/how-should-we-assess-security-and-data-minimisation-in-ai/>. Ac-  
579 cessed: 2025-09-17.

580 Bogdan Kulynych, Mohammad Yaghini, Giovanni Cherubin, Michael Veale, and Carmela Troncoso.  
581 Disparate vulnerability to membership inference attacks. *Proceedings on Privacy Enhancing*  
582 *Technologies*, 1:460–480, 2022.

583 Tobias Leemann, Bardh Prenkaj, and Gjergji Kasneci. Is my data safe? predicting instance-level  
584 membership inference success for white-box and black-box attacks. In *ICML 2024 Next Genera-*  
585 *tion of AI Safety Workshop*, 2024.

594 Hao Li, Zheng Li, Siyuan Wu, Chengrui Hu, Yutong Ye, Min Zhang, Dengguo Feng, and Yang  
595 Zhang. Seqmia: sequential-metric based membership inference attack. In *Proceedings of the*  
596 *2024 on ACM SIGSAC Conference on Computer and Communications Security*, pp. 3496–3510,  
597 2024.

598 Yiyong Liu, Zhengyu Zhao, Michael Backes, and Yang Zhang. Membership inference attacks by  
599 exploiting loss trajectory. In *Proceedings of the 2022 ACM SIGSAC Conference on Computer and*  
600 *Communications Security*, CCS ’22, pp. 2085–2098, New York, NY, USA, 2022. Association for  
601 Computing Machinery. ISBN 9781450394505. doi: 10.1145/3548606.3560684. URL <https://doi.org/10.1145/3548606.3560684>.

602 Justus Mattern, Fatemehsadat Mireshghallah, Zhijing Jin, Bernhard Schölkopf, Mrinmaya Sachan,  
603 and Taylor Berg-Kirkpatrick. Membership inference attacks against language models via neigh-  
604 borhood comparison, 2023. URL <https://arxiv.org/abs/2305.18462>.

605 Gergely Dániel Németh, Miguel Ángel Lozano, Novi Quadrianto, and Nuria Oliver. Privacy and  
606 accuracy implications of model complexity and integration in heterogeneous federated learning,  
607 2025. URL <https://arxiv.org/abs/2311.17750>.

608 Joseph Pollock, Igor Shilov, Euodia Dodd, and Yves-Alexandre de Montjoye. Free {Record-Level}  
609 privacy risk evaluation through {Artifact-Based} methods. In *34th USENIX Security Symposium*  
610 (*USENIX Security 25*), pp. 5525–5544, 2025.

611 Natalia Ponomareva, Sergei Vassilvitskii, Zheng Xu, Brendan McMahan, Alexey Kurakin, and  
612 Chiyaun Zhang. How to dp-fy ml: A practical tutorial to machine learning with differen-  
613 tial privacy. In *Proceedings of the 29th ACM SIGKDD Conference on Knowledge Discov-  
614 ery and Data Mining*, KDD ’23, pp. 5823–5824, New York, NY, USA, 2023. Association for  
615 Computing Machinery. ISBN 9798400701030. doi: 10.1145/3580305.3599561. URL  
616 <https://doi.org/10.1145/3580305.3599561>.

617 Mark Sandler, Andrew Howard, Menglong Zhu, Andrey Zhmoginov, and Liang-Chieh Chen. Mo-  
618 bilenetv2: Inverted residuals and linear bottlenecks. In *Proceedings of the IEEE conference on*  
619 *computer vision and pattern recognition*, pp. 4510–4520, 2018.

620 Igor Shilov, Matthieu Meeus, and Yves-Alexandre de Montjoye. The mosaic memory of large  
621 language models. *arXiv preprint arXiv:2405.15523*, 2024.

622 Reza Shokri, Marco Stronati, Congzheng Song, and Vitaly Shmatikov. Membership inference at-  
623 tacks against machine learning models. In *2017 IEEE symposium on security and privacy (SP)*,  
624 pp. 3–18. IEEE, 2017.

625 K Simonyan and A Zisserman. Very deep convolutional networks for large-scale image recognition.  
626 In *3rd International Conference on Learning Representations (ICLR 2015)*. Computational and  
627 Biological Learning Society, 2015.

628 Liwei Song and Prateek Mittal. Systematic evaluation of privacy risks of machine learning models,  
629 2020. URL <https://arxiv.org/abs/2003.10595>.

630 Liwei Song, Reza Shokri, and Prateek Mittal. Privacy risks of securing machine learning models  
631 against adversarial examples. In *Proceedings of the 2019 ACM SIGSAC conference on computer*  
632 *and communications security*, pp. 241–257, 2019.

633 Kushal Tirumala, Aram Markosyan, Luke Zettlemoyer, and Armen Aghajanyan. Memorization  
634 without overfitting: Analyzing the training dynamics of large language models. *Advances in*  
635 *Neural Information Processing Systems*, 35:38274–38290, 2022.

636 Marlon Tobaben, Hibiki Ito, Joonas Jälkö, Yuan He, and Antti Honkela. Impact of dataset properties  
637 on membership inference vulnerability of deep transfer learning, 2025. URL <https://arxiv.org/abs/2402.06674>.

638 Lauren Watson, Chuan Guo, Graham Cormode, and Alex Sablayrolles. On the importance of diffi-  
639 culty calibration in membership inference attacks. *arXiv preprint arXiv:2111.08440*, 2021.

648  
 649  
 650  
 651  
 652  
 653  
 654  
 655  
 656  
 657  
 658  
 659  
 660  
 661  
 662  
 663  
 664  
 665  
 666  
 667  
 668  
 669  
 670  
 671  
 672  
 673  
 674  
 675  
 676  
 677  
 678  
 679  
 680  
 681  
 682  
 683  
 684  
 685  
 686  
 687  
 688  
 689  
 690  
 691  
 692  
 693  
 694  
 695  
 696  
 697  
 698  
 699  
 700  
 701  
 Jiayuan Ye, Aadyaa Maddi, Sasi Kumar Murakonda, Vincent Bindschaedler, and Reza Shokri. Enhanced membership inference attacks against machine learning models. In *Proceedings of the 2022 ACM SIGSAC conference on computer and communications security*, pp. 3093–3106, 2022.

Samuel Yeom, Irene Giacomelli, Matt Fredrikson, and Somesh Jha. Privacy risk in machine learning: Analyzing the connection to overfitting. In *2018 IEEE 31st computer security foundations symposium (CSF)*, pp. 268–282. IEEE, 2018.

Sergey Zagoruyko and Nikos Komodakis. Wide residual networks. *arXiv preprint arXiv:1605.07146*, 2016.

Sajjad Zarifzadeh, Philippe Liu, and Reza Shokri. Low-cost high-power membership inference attacks. *arXiv preprint arXiv:2312.03262*, 2023.

## 8 APPENDIX

### A LOSS DISTRIBUTIONS ACROSS ALL SETUPS

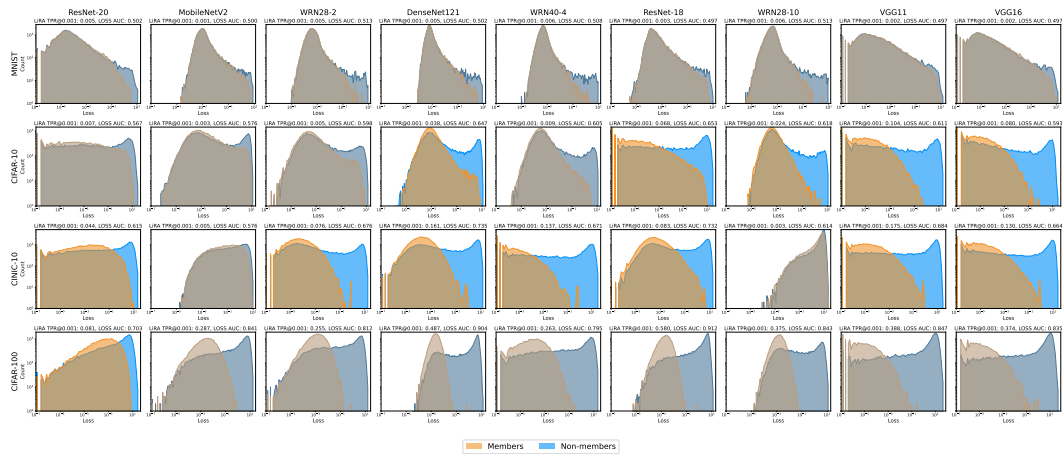


Figure 8: Histograms showing  $\ell_{\text{target}}$  distributions for training set members (orange) and non-members (blue) in log-log scale across all setups. The distributions demonstrate clear separation between members and non-members, with members typically having lower loss values.

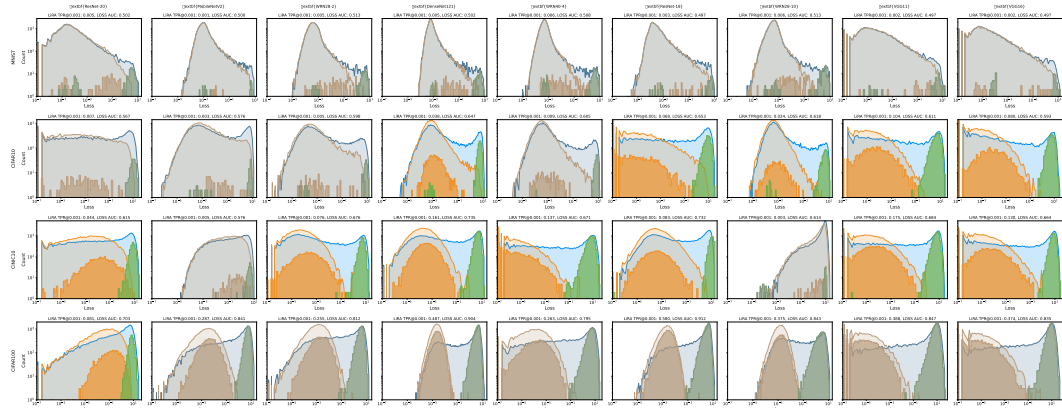


Figure 9:  $\ell_{\text{target}}$  distributions for training set members and non-members across all setups. Orange histogram shows member losses, blue shows non-member losses, with density curves overlaid. Green bars indicate the OUT model mean ( $\ell_{\text{out}}$ ) for points identified by LiRA at  $\text{FPR}=0.001$ .

---

## B VARYING FPRs

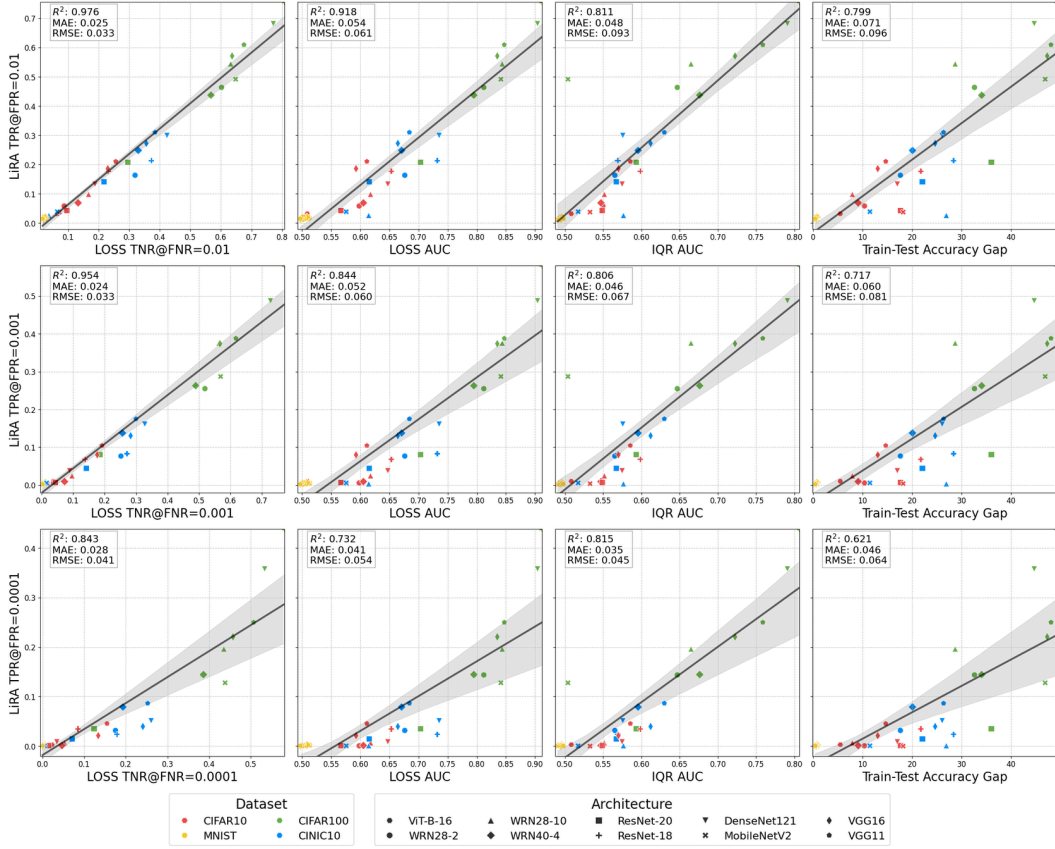


Figure 10: Comparison of different metrics for predicting LiRA TPR at FPRs of 0.01, 0.001, 0.0001. Each panel shows the relationship between a predictor metric (x-axis) and LiRA TPR (y-axis) across all model-dataset combinations. Linear fits (solid lines) with 97.5% confidence intervals (shaded regions) show goodness-of-fit.

## C SENSITIVITY TO SELECTION OF LOSS FNR THRESHOLD

We select  $\text{FPR}=\text{FNR}$  across the paper, as it is a natural choice. We here study the sensitivity of LOSS TNR’s predictive capability to the choice of FNR threshold. Following the experimental setup described in Section 3, we evaluate how well LOSS TNR predicts LiRA’s TPR across four different false positive rate thresholds: 0.1, 0.01, 0.001, and 0.0001. For each LiRA FPR setting, we fit a linear function to predict the corresponding LiRA TPR from LOSS TNR values computed at varying FNR thresholds, and measure prediction quality using the RMSE.

Figure 11 shows that RMSE remains relatively stable across a broad range of FNR values, demonstrating that LOSS TNR’s predictive power is robust to the specific threshold selection. Notably, setting the FNR equal to the target LiRA FPR (green stars) achieves a similar performance compared to the FNR that minimizes RMSE (yellow stars), showing it to be a good and principled choice. The sharp degradation in RMSE only occurs at very high FNR values (approaching 1.0), where the LOSS threshold becomes too relaxed to provide a meaningful signal.

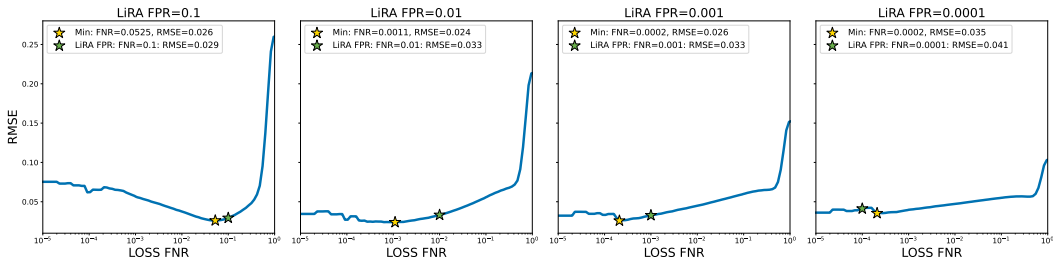


Figure 11: RMSE of LOSS TNR@different FNR values as a predictor of LiRA TPR at a fixed FPR. The yellow star indicates the FNR that achieves the lowest RMSE, while the green star shows performance when setting the FNR to equal to the LiRA FPR. Across all settings, the RMSE difference between the optimal selection and FNR=FPR is minimal.

## D EXTENDED INTUITION

We provide a formal explanation of the connection between LiRA TPR@FPR and the LOSS attack TNR@FNR. For a record  $(x, y)$ , we use the notation from Section 4 for the mean IN and OUT losses,  $\ell_{\text{in}}$  and  $\ell_{\text{out}}$ .

Consider a target model  $f_\theta \leftarrow \mathcal{T}(D_{\text{train}})$ . We refer to records contained in  $D_{\text{train}}$ , i.e., records the model has seen during training, as *members*, and to records in  $D_{\text{test}}$ , i.e., records the model has not seen during training, as *non-members*.

For a record  $(x, y)$ , we denote  $Q_{\text{in}}$  and  $Q_{\text{out}}$  the distributions of its IN and OUT losses, respectively, and denote its LiRA score by  $\Lambda(x, y)$ .

For a member  $(x, y)$ , if  $Q_{\text{in}}$  and  $Q_{\text{out}}$  differ substantially, training the model on  $(x, y)$  has a large effect on its loss on  $(x, y)$ : the loss typically moves from high values (in the tail of the loss distribution) to low values (in the head). In this case,  $\Lambda(x, y)$  is likely to be high, making  $(x, y)$  highly vulnerable to LiRA. We call such records *tail-to-head* records and denote the set of all such training records by  $D_{\text{th}}$ .

At some LiRA threshold  $\tau_{\text{LiRA}}$ ,  $D_{\text{th}}$  makes up a fraction  $\alpha$  of the highly vulnerable records in  $D_{\text{train}}$ :

$$|D_{\text{th}}| = \alpha \left| \{(x, y) \in D_{\text{train}} : \Lambda(x, y) \geq \tau_{\text{LiRA}}\} \right|, \quad (5)$$

$$\frac{|D_{\text{th}}|}{|D_{\text{train}}|} = \alpha \frac{\left| \{(x, y) \in D_{\text{train}} : \Lambda(x, y) \geq \tau_{\text{LiRA}}\} \right|}{|D_{\text{train}}|}. \quad (6)$$

The quantity on the right-hand side of the second line is precisely the LiRA true positive rate at threshold  $\tau_{\text{LiRA}}$ , i.e.,

$$\frac{|D_{\text{th}}|}{|D_{\text{train}}|} = \alpha \text{TPR}_{\text{LiRA}}(\tau_{\text{LiRA}}). \quad (7)$$

Thus, the LiRA TPR is proportional to the fraction of tail-to-head records in  $D_{\text{train}}$ , and this fraction characterizes model-level vulnerability.

We now consider the records in  $D_{\text{test}}$ . Records in  $D_{\text{test}}$  that lie in the tail of the loss distribution under  $f_\theta$  are likely to have high OUT loss, i.e., large loss when they are not seen during training. If we were to train on such a record, its loss would either (i) remain in the tail (the model does not learn it) or (ii) move to the head (the model memorizes it). Empirically, training loss distributions are typically not heavy-tailed. We therefore assume that most records in  $D_{\text{test}}$  that are in the tail of the OUT-loss distribution would move to the head if they were included in training. These are the analogous to the tail-to-head records in  $D_{\text{train}}$ .

Assuming that  $D_{\text{train}}$  and  $D_{\text{test}}$  are drawn i.i.d. from the same underlying distribution, we can estimate the fraction of tail-to-head records in  $D_{\text{train}}$  by the corresponding fraction of tail records in  $D_{\text{test}}$  at

some LOSS threshold  $\tau_{\text{LOSS}}$ :

$$\frac{|\{(x, y) \in D_{\text{test}} : \ell_{\text{out}}(x, y) \geq \tau_{\text{LOSS}}\}|}{|D_{\text{test}}|} = \frac{|D_{\text{th}}|}{|D_{\text{train}}|} + \varepsilon, \quad (8)$$

for some small error term  $\varepsilon$ .

The left-hand side is exactly the TNR of the LOSS attack at threshold  $\tau_{\text{LOSS}}$ . Hence,

$$\text{TNR}_{\text{LOSS}}(\tau_{\text{LOSS}}) = \alpha \text{TPR}_{\text{LiRA}}(\tau_{\text{LiRA}}) + \varepsilon. \quad (9)$$

This formalizes the intuition that the LOSS TNR provides a linear proxy for the LiRA TPR, up to a proportionality constant  $\alpha$  and an error term  $\varepsilon$ .

## E PREDICTING VULNERABILITY TO DIFFERENT ATTACKS

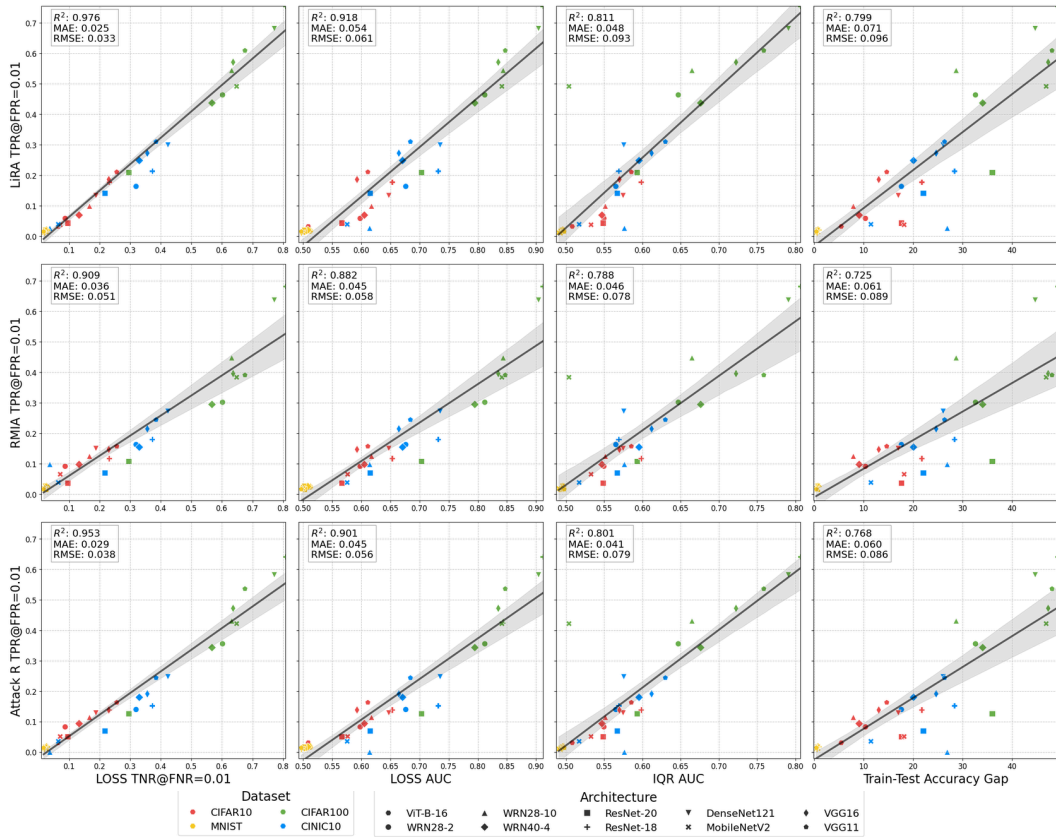


Figure 12: Comparison of different metrics for predicting the TPR at  $\text{FPR}=0.01$  for LiRA, RMIA and Attack-R with 64 reference models. Each panel shows the relationship between a predictor metric (x-axis) and the attack TPR (y-axis) across all model-dataset combinations. Linear fits (solid lines) with 97.5% confidence intervals (shaded regions) show goodness-of-fit.

To evaluate whether our method generalizes to other attacks within the same family, we estimate the TPR@0.01 for RMIA and Attack R using 64 reference models (for RMIA: 32 IN and 32 OUT; for Attack R: 64 OUT). Figure N demonstrates that TNR serves as an effective predictor for both RMIA and Attack R (two reference-model-based MIAs). Since these attacks share a common approach of using reference models to estimate counterfactuals for individual samples, it follows logically that TNR captures the same underlying signal across attacks in this family.